Available online at www.sciencedirect.com
SCIENCE DIRECT®
ELSEVIER
Engineering Structures 27 (2005) 1185–1196
ENGINEERING STRUCTURES
www.elsevier.com/locate/engstruct

Lateral buckling of thin-walled composite bisymmetric beams with prebuckling and shear deformation

Sebastián P. Machado[a,b], Víctor H. Cortínez[a,b,*]

[a] *Grupo Análisis de Sistemas Mecánicos, Facultad Regional Bahía Blanca, Universidad Tecnológica Nacional, 11de abril 461, B8000LMI Bahía Blanca, Argentina*
[b] *CONICET, Argentina*

Received 15 November 2004; received in revised form 23 February 2005; accepted 28 February 2005
Available online 10 May 2005

Abstract

The effects of the in-plane prebuckling deformations as well as the effect of shear flexibility on the lateral buckling of bisymmetric thin-walled composite beams has been investigated in this paper. The analysis is based on a geometrically non-linear theory based on large displacements and rotations. The Ritz variational method is used in order to discretize the governing equation and then the buckling loads are obtained by requiring the singularity of the tangential stiffness matrix. The numerical results show that the classical predictions of lateral buckling are inaccurate, and the considered effects should be taken into account for obtaining reliable solutions. Besides, the effects of span length and height of the load point have also been investigated for different laminate stacking sequence.

Keywords: Thin-walled beams; Shear flexibility; Composite material; Prebuckling

1. Introduction

Structural members made of composites are increasingly used in aeronautical, mechanical and civil engineering applications where high strength and stiffness, and low weight are of primary importance. Many structural members made of composites have the form of thin-walled beams. These kinds of members are the most common load-carrying systems in engineering applications. When loaded in its plane of symmetry, the beam initially deflects. However, at a certain level of the applied load, the beam may buckle laterally, while its cross-section rotates simultaneously about the beam's axis. This phenomenon is called lateral buckling, and the value of the load at which buckling occurs is the critical load. Therefore, the accurate prediction of the stability limit state is of fundamental importance in the design of thin-walled structures. Several studies of lateral buckling of thin-walled beams have been developed by using a linearized approach based on Vlasov's theory. In this way, buckling loads were determined for thin-walled beams made of metallic [1–6] and composite materials (for example: [7,8]). The limitation of the linear buckling analysis of beams [1] is the omission of any consideration of the effect of prebuckling deflections. This omission may lead to inaccurate results when the prebuckling deflections of the beam are not negligible.

On the other hand, a few closed-form solutions have been obtained for critical loads considering the prebuckling deflections of the beam [9–13].

The shear deformation effect has not been considered in the last five references. However, it is well known that this effect plays an important role in the behavior of linear stability of thin-walled composite beams, owing to the high ratio between the equivalent elasticity modulus and transverse elasticity modulus [7,14].

* Corresponding author at: Grupo Análisis de Sistemas Mecánicos, Facultad Regional Bahía Blanca, Universidad Tecnológica Nacional, 11de abril 461, B8000LMI Bahía Blanca, Argentina. Tel.: +54 0291 4555220; fax: +54 0291 4555311.
E-mail addresses: smachado@frbb.utn.edu.ar (S.P. Machado), vcortine@frbb.utn.edu.ar (V.H. Cortínez).

0141-0296/$ - see front matter © 2005 Elsevier Ltd. All rights reserved.
doi:10.1016/j.engstruct.2005.02.018

In this paper a geometrically non-linear beam theory is presented that takes into account several non-classical effects, such as shear flexibility. On the other hand, it is valid for symmetric balanced laminates and especially orthotropic laminates [15,16]. The primary purpose of this paper is to investigate numerically the effects of the prebuckling displacements as well as the effect of shear deformation on the lateral buckling of bisymmetric thin-walled composite beams subjected to concentrated end moments, concentrated forces, or uniformly distributed load. Simply supported and cantilever beams are considered.

A second purpose is to investigate the effects of span length and the load height on the lateral buckling for different laminate stacking sequences.

In order to perform the analysis, the Ritz variational method [17] is used for reducing the governing equation in terms of generalized coordinates. From the reduced system, the buckling loads are determined from the singularity condition of the tangential stiffness matrix evaluated in the fundamental state. In this way the prebuckling deformations are taken into account avoiding the employment of a full non-linear analysis. Moreover, for the case of simply supported ends, a simple analytical formula for the critical loads is obtained. The results thus determined are compared with values obtained by means of the linearized theory in order to evaluate the importance of the effects taken into account.

2. Kinematics

A straight thin-walled composite beam with an arbitrary cross-section is considered (Fig. 1). The points of the structural member are referred to a Cartesian co-ordinate system $(x, \bar{y}, \bar{z})$, where the x-axis is parallel to the longitudinal axis of the beam while $\bar{y}$ and $\bar{z}$ are the principal axes of the cross-section. The axes y and z are parallel to the principal ones but having their origin at the shear center (defined according to Vlasov's theory of isotropic beams). The co-ordinates corresponding to points lying on the middle line are denoted as Y and Z (or $\overline{Y}$ and $\overline{Z}$). In addition, a circumferential co-ordinate s and a normal co-ordinate n are introduced on the middle contour of the cross-section.

$$\bar{y}(s,n) = \overline{Y}(s) - n\frac{dZ}{ds}, \qquad \bar{z}(s,n) = \overline{Z}(s) + n\frac{dY}{ds} \tag{1}$$

$$y(s,n) = Y(s) - n\frac{dZ}{ds}, \qquad z(s,n) = Z(s) + n\frac{dY}{ds}. \tag{2}$$

On the other hand, y_0 and z_0 are the centroidal co-ordinates measured with respect to the shear center.

$$\begin{aligned} \bar{y}(s,n) &= y(s,n) - y_0 \\ \bar{z}(s,n) &= z(s,n) - z_0. \end{aligned} \tag{3}$$

The present structural model is based on the following assumptions [14]:

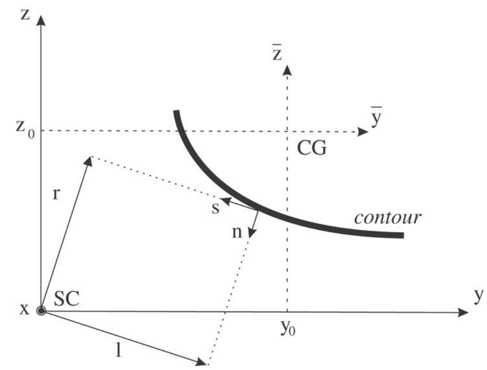

Fig. 1. Co-ordinate system of the cross-section.

(1) The cross-section contour is rigid in its own plane.
(2) The warping distribution is assumed to be given by the Saint-Venant function for isotropic beams.
(3) Flexural rotations (about the $\bar{y}$ and $\bar{z}$ axes) are assumed to be moderate, while the twist ϕ of the cross-section can be arbitrarily large.
(4) Shell force and moment resultant corresponding to the circumferential stress σ_{ss} and the force resultant corresponding to γ_{ns} are neglected.
(5) The radius of curvature at any point of the shell is neglected.
(6) Twisting linear curvature of the shell is expressed according to the classical plate theory.
(7) The laminate stacking sequence is assumed to be symmetric and balanced, or especially orthotropic [15, 16].

According to these hypotheses the displacement field is assumed to be in the following form

$$\begin{aligned} u_x &= u_o - \bar{y}(\theta_z\cos\phi + \theta_y\sin\phi) - \bar{z}(\theta_y\cos\phi - \theta_z\sin\phi) \\ &\quad + \omega\left[\theta \underline{- \frac{1}{2}(\theta_y'\theta_z - \theta_y\theta_z')}\right] + (\theta_z z_0 - \theta_y y_0)\sin\phi \\ u_y &= v - z\sin\phi - y(1-\cos\phi) \underline{- \frac{1}{2}(\theta_z^2\bar{y} + \theta_z\theta_y\bar{z})} \\ u_z &= w + y\sin\phi - z(1-\cos\phi) \underline{- \frac{1}{2}(\theta_y^2\bar{z} + \theta_z\theta_y\bar{y})}. \end{aligned} \tag{4}$$

This expression is a generalization of others previously proposed in the literature.

The displacement field proposed by Fraternali and Feo [18] is recovered (see Appendix A) by considering $\theta_z = v', \theta_y = w'$ and $\theta = \phi'$ (neglecting flexural and torsional shear flexibility), approximating $\cos\phi$ and $\sin\phi$ by $(1 - \phi^2/2)$ and ϕ respectively, and conserving non-linear terms up to second order. Moreover, the displacement field of the classical Vlasov theory is obtained when second-order effects are ignored.

On the other hand, a simplified analog of Eqs. (4), disregarding the underlined terms and shear flexibility, was used by Mohri [13].

As a final comparison, taking $\cos\phi = 1$ and $\sin\phi = \phi$ and disregarding the non-linear terms, the displacement field (4) coincides with the one formulated by Cortínez and Piovan [14] for linear dynamics of shear deformable thin-walled beams.

In the above expressions ϕ, θ_y and θ_z are measures of the rotations about the shear center axis, $\bar{y}$ and $\bar{z}$ axes, respectively; θ represents the warping variable of the cross-section. Furthermore the superscript 'prime' denotes derivation with respect to the variable x. The warping function ω of the thin-walled cross-section may be defined as:

$$\omega(s,n) = \omega_p(s) + \omega_s(s,n) \tag{5}$$

where ω_p and ω_s are the contour warping function and the thickness warping function, respectively. They are defined in the form [19]:

$$\begin{aligned} \omega_p(s) &= \frac{1}{S}\left[\int_0^S \left(\int_{s_0}^s [r(s)-\psi(s)]\mathrm{d}s\right)\mathrm{d}s\right] \\ &\quad - \int_{s_0}^s [r(s)-\psi(s)]\mathrm{d}s \\ \omega_s(s,n) &= -nl(s) \end{aligned} \tag{6}$$

where

$$r(s) = -Z(s)\frac{\mathrm{d}Y}{\mathrm{d}s} + Y(s)\frac{\mathrm{d}Z}{\mathrm{d}s} \tag{7}$$

$$l(s) = Y(s)\frac{\mathrm{d}Y}{\mathrm{d}s} + Z(s)\frac{\mathrm{d}Z}{\mathrm{d}s} \tag{8}$$

$r(s)$ represents the perpendicular distance from the shear center (SC) to the tangent at any point of the mid-surface contour, and $l(s)$ represents the perpendicular distance from the shear center (SC) to the normal at any point of the mid-surface contour, as shown in Fig. 1.

In the expression (6) Ψ is the shear strain at the middle line, obtained by means of the Saint-Venant theory of pure torsion for isotropic beams, and normalized with respect to $\mathrm{d}\phi/\mathrm{d}x$ [20]. For the case of open sections $\Psi = 0$.

3. The strain field

The displacements with respect to the curvilinear system (x, s, n) are obtained by means of the following expressions:

$$\overline{U} = u_x(x,s,n) \tag{9}$$

$$\overline{V} = u_y(x,s,n)\frac{\mathrm{d}Y}{\mathrm{d}s} + u_z(x,s,n)\frac{\mathrm{d}Z}{\mathrm{d}s} \tag{10}$$

$$\overline{W} = -u_y(x,s,n)\frac{\mathrm{d}Z}{\mathrm{d}s} + u_z(x,s,n)\frac{\mathrm{d}Y}{\mathrm{d}s}. \tag{11}$$

The three non-zero components $\varepsilon_{xx}, \varepsilon_{xs}, \varepsilon_{xn}$ of the Green's strain tensor are given by:

$$\varepsilon_{xx} = \frac{\partial\overline{U}}{\partial x} + \frac{1}{2}\left[\left(\frac{\partial\overline{U}}{\partial x}\right)^2 + \left(\frac{\partial\overline{V}}{\partial x}\right)^2 + \left(\frac{\partial\overline{W}}{\partial x}\right)^2\right] \tag{12}$$

$$\varepsilon_{xs} = \frac{1}{2}\left[\frac{\partial\overline{U}}{\partial s} + \frac{\partial\overline{V}}{\partial x} + \frac{\partial\overline{U}}{\partial x}\frac{\partial\overline{U}}{\partial s} + \frac{\partial\overline{V}}{\partial x}\frac{\partial\overline{V}}{\partial s} + \frac{\partial\overline{W}}{\partial x}\frac{\partial\overline{W}}{\partial s}\right] \tag{13}$$

$$\varepsilon_{xn} = \frac{1}{2}\left[\frac{\partial\overline{U}}{\partial n} + \frac{\partial\overline{W}}{\partial x} + \frac{\partial\overline{U}}{\partial x}\frac{\partial\overline{U}}{\partial n} + \frac{\partial\overline{V}}{\partial x}\frac{\partial\overline{V}}{\partial n} + \frac{\partial\overline{W}}{\partial x}\frac{\partial\overline{W}}{\partial n}\right]. \tag{14}$$

Substituting expressions (4) into (9)–(11) and then into (12)–(14), employing the relations (1)–(3) and (5)–(8), after simplifying some higher order terms, the components of the strain tensor are expressed in the following form:

$$\begin{aligned} \varepsilon_{xx} &= \varepsilon_{xx}^{(0)} + n\kappa_{xx}^{(1)} \\ \gamma_{xs} &= 2\varepsilon_{xs} = \gamma_{xs}^{(0)} + n\kappa_{xs}^{(1)} \\ \gamma_{xn} &= 2\varepsilon_{xn} = \gamma_{xn}^{(0)} \end{aligned} \tag{15}$$

where

$$\begin{aligned} \varepsilon_{xx}^{(0)} &= u_o' + \frac{1}{2}(v'^2 + w'^2) + \omega_p\left[\theta' - \frac{1}{2}(\theta_z\theta_y'' - \theta_y\theta_z'')\right] \\ &\quad + \overline{Z}(-\theta_y'\cos\phi + \theta_z'\sin\phi) + \overline{Y}(-\theta_z'\cos\phi \\ &\quad - \theta_y'\sin\phi) + \frac{1}{2}\phi'^2(Y^2+Z^2) + (z_0\theta_z' - y_0\theta_y')\sin\phi \\ &\quad + \phi'(z_0\theta_z - y_0\theta_y)\cos\phi \end{aligned} \tag{16}$$

$$\begin{aligned} \kappa_{xx}^{(1)} &= -\frac{\mathrm{d}Z}{\mathrm{d}s}(-\theta_z'\cos\phi - \theta_y'\sin\phi) + \frac{\mathrm{d}Y}{\mathrm{d}s}(-\theta_y'\cos\phi \\ &\quad + \theta_z'\sin\phi) - l\left[\theta' - \frac{1}{2}(\theta_z\theta_y'' - \theta_y\theta_z'')\right] - r\phi'^2 \end{aligned} \tag{17}$$

$$\begin{aligned} \gamma_{xs}^{(0)} &= \frac{\mathrm{d}Y}{\mathrm{d}s}\left[(v' - \theta_z)\cos\phi - z_0\frac{1}{2}(\theta_z\theta_y' - \theta_y\theta_z') \right. \\ &\quad \left. + (w' - \theta_y)\sin\phi\right] + (r - \psi)(\phi' - \theta) \\ &\quad + \frac{\mathrm{d}Z}{\mathrm{d}s}\left[(w' - \theta_y)\cos\phi + y_0\frac{1}{2}(\theta_z\theta_y' - \theta_y\theta_z') \right. \\ &\quad \left. - (v' - \theta_z)\sin\phi\right] + \psi\left[\phi' - \frac{1}{2}(\theta_z\theta_y' - \theta_y\theta_z')\right] \end{aligned} \tag{18}$$

$$\kappa_{xs}^{(1)} = -2\left[\phi' - \frac{1}{2}(\theta_z\theta_y' - \theta_y\theta_z')\right] \tag{19}$$

$$\begin{aligned} \gamma_{xn}^{(0)} &= \frac{\mathrm{d}Y}{\mathrm{d}s}\left[(w' - \theta_y)\cos\phi + y_0\frac{1}{2}(\theta_z\theta_y' - \theta_y\theta_z') \right. \\ &\quad \left. - (v' - \theta_z)\sin\phi\right] - \frac{\mathrm{d}Z}{\mathrm{d}s}\left[(v' - \theta_z)\cos\phi \right. \\ &\quad \left. - z_0\frac{1}{2}(\theta_z\theta_y' - \theta_y\theta_z') + (w' - \theta_y)\sin\phi\right] \\ &\quad + l(\phi' - \theta). \end{aligned} \tag{20}$$

4. Variational formulation

Taking into account the adopted assumptions, the principle of virtual work for a composite shell may be expressed in the form [21,14]:

$$\begin{aligned}
&\iint (N_{xx}\delta\varepsilon_{xx}^{(0)} + M_{xx}\delta\kappa_{xx}^{(1)} + N_{xs}\delta\gamma_{xs}^{(0)} \\
&\quad + M_{xs}\delta\kappa_{xs}^{(1)} + N_{xn}\delta\gamma_{ns}^{(0)})\,\mathrm{d}s\,\mathrm{d}x \\
&- \iint (\bar{q}_x\delta\bar{u}_x + \bar{q}_y\delta\bar{u}_y + \bar{q}_z\delta\bar{u}_z)\,\mathrm{d}s\,\mathrm{d}x \\
&\quad - \iint (\bar{p}_x\delta u_x + \bar{p}_y\delta u_y + \bar{p}_z\delta u_z)|_{x=0}\,\mathrm{d}s\,\mathrm{d}n \\
&- \iint (\bar{p}_x\delta u_x + \bar{p}_y\delta u_y + \bar{p}_z\delta u_z)|_{x=L}\,\mathrm{d}s\,\mathrm{d}n \\
&\quad - \iiint (\bar{f}_x\delta u_x + \bar{f}_y\delta u_y + \bar{f}_z\delta u_z)\,\mathrm{d}s\,\mathrm{d}n\,\mathrm{d}x = 0
\end{aligned} \tag{21}$$

where $N_{xx}, N_{xs}, M_{xx}, M_{xs}$ and N_{xn} are the shell stress resultants defined according to the following expressions:

$$\begin{aligned}
N_{xx} &= \int_{-e/2}^{e/2} \sigma_{xx}\,\mathrm{d}n; \qquad M_{xx} = \int_{-e/2}^{e/2} (\sigma_{xx} n)\,\mathrm{d}n; \\
N_{xs} &= \int_{-e/2}^{e/2} \sigma_{xs}\,\mathrm{d}n; \qquad M_{xs} = \int_{-e/2}^{e/2} (\sigma_{xs} n)\,\mathrm{d}n; \\
N_{xn} &= \int_{-e/2}^{e/2} \sigma_{xn}\,\mathrm{d}n.
\end{aligned} \tag{22}$$

The beam is subjected to wall surface tractions $\bar{q}_x, \bar{q}_y$ and $\bar{q}_z$ specified per unit area of the undeformed middle surface and acting along the x, y and z directions, respectively. Similarly, $\bar{p}_x$, $\bar{p}_y$ and $\bar{p}_z$ are the end tractions per unit area of the undeformed cross-section specified at $x = 0$ and $x = L$, where L is the undeformed length of the beam. Besides $\bar{f}_x$, $\bar{f}_y$ and $\bar{f}_z$ are the body forces per unit of volume. Finally, denoting $\bar{u}_x, \bar{u}_y$ and $\bar{u}_z$ as displacements at the middle line.

5. Constitutive equations

The constitutive equations of symmetrically balanced laminates may be expressed in the terms of shell stress resultants in the following form [15]:

$$\begin{Bmatrix} N_{xx} \\ N_{xs} \\ N_{xn} \\ M_{xx} \\ M_{xs} \end{Bmatrix} = \begin{bmatrix} \overline{A}_{11} & 0 & 0 & 0 & 0 \\ 0 & \overline{A}_{66} & 0 & 0 & 0 \\ 0 & 0 & \overline{A}_{55}^{(H)} & 0 & 0 \\ 0 & 0 & 0 & \overline{D}_{11} & 0 \\ 0 & 0 & 0 & 0 & \overline{D}_{66} \end{bmatrix} \begin{Bmatrix} \varepsilon_{xx}^{(0)} \\ \gamma_{xs}^{(0)} \\ \gamma_{xn}^{(0)} \\ \kappa_{xx}^{(1)} \\ \kappa_{xs}^{(1)} \end{Bmatrix} \tag{23}$$

with

$$\begin{aligned}
&\overline{A}_{11} = A_{11} - \frac{A_{12}^2}{A_{22}}, \qquad \overline{A}_{66} = A_{66} - \frac{A_{26}^2}{A_{22}}, \\
&\quad \overline{A}_{55}^{(H)} = A_{55}^{(H)} - \frac{(A_{45}^{(H)})^2}{A_{44}^{(H)}} \\
&\overline{D}_{11} = D_{11} - \frac{D_{12}^2}{D_{22}}, \qquad \overline{D}_{66} = D_{66} - \frac{D_{26}^2}{D_{22}}
\end{aligned} \tag{24}$$

where A_{ij}, D_{ij} and $A_{ij}^{(H)}$ are plate stiffness coefficients defined according to the lamination theory presented by Barbero [15]. The coefficient $\overline{D}_{16}$ has been neglected because of its low value for the considered laminate stacking sequence [14].

6. Principle of virtual work for thin-walled beams

Substituting expressions (16)–(20) into (21) and integrating with respect to s, one obtains the one-dimensional expression for the virtual work equation given by:

$$L_K + L_P = 0 \tag{25}$$

where, L_k and L_p represent the virtual work contributions due to the internal and external forces, respectively. Their expressions are given below.

$$\begin{aligned}
L_K = \int_0^L \Big\{ & \delta u_0' N + \delta v'(Q_y \cos\phi - Q_z \sin\phi + v'N) \\
& + \delta w'(Q_z \cos\phi + Q_y \sin\phi + w'N) \\
& + \delta\theta_z \Big[-Q_y \cos\phi + Q_z \sin\phi + \frac{1}{2}(Q_z y_0 - Q_y z_0)\theta_y' \\
& - \frac{1}{2} T_{sv}\theta_y' - \frac{1}{2} B\theta_y'' + N\phi' z_0 \cos\phi \Big] \\
& + \delta\theta_z' \Big[-M_z \cos\phi + (M_y + N z_0)\sin\phi + \frac{1}{2}(Q_y z_0 \\
& - Q_z y_0)\theta_y + \frac{1}{2} T_{sv}\theta_y \Big] + \delta\theta_z'' \frac{1}{2} B\theta_y \\
& + \delta\theta_y \Big[-Q_z \cos\phi - Q_y \sin\phi + \frac{1}{2}(Q_y z_0 - Q_z y_0)\theta_z' \\
& + \frac{1}{2} T_{sv}\theta_z' + \frac{1}{2} B\theta_z'' - N\phi' y_0 \cos\phi \Big] \\
& + \delta\theta_y' \Big[-M_y \cos\phi - (M_z + N y_0)\sin\phi + \frac{1}{2}(Q_z y_0 \\
& - Q_y z_0)\theta_z - \frac{1}{2} T_{sv}\theta_z \Big] - \delta\theta_y'' \frac{1}{2} B\theta_z \\
& + \delta\phi [M_y(\theta_y' \sin\phi + \theta_z' \cos\phi) + M_z(\theta_z' \sin\phi \\
& - \theta_y' \cos\phi) + N(z_0\theta_z' - y_0\theta_y')\cos\phi \\
& - N\phi'(z_0\theta_z - y_0\theta_y)\sin\phi \\
& + Q_y((\theta_z - v')\sin\phi - (\theta_y - w')\cos\phi) \\
& + Q_z((\theta_y - w')\sin\phi + (\theta_z - v')\cos\phi)] \\
& + \delta\phi'[T_w + T_{sv} + B_1\phi' \\
& + N(\theta_z z_0 - \theta_y y_0)\cos\phi] + \delta\theta' B - \delta\theta T_w \Big\}\,\mathrm{d}x.
\end{aligned} \tag{26}$$

In the present study, the lateral buckling of beams initially loaded in bending about the principal axis is considered. Thus, the external work L_p is defined by the following relationship:

$$L_P = \int_0^L (-q_z\delta w + \delta\phi\phi e_z q_z)\mathrm{d}x + |\delta\theta_y \overline{M}_y|_{x=0}^{x=L} \tag{27}$$

where

$$q_z = \int \bar{q}_z \mathrm{d}s + \iint \bar{f}_z \mathrm{d}s\ \mathrm{d}n, \quad \overline{M}_y = \iint \bar{p}_x \bar{z}\ \mathrm{d}s\ \mathrm{d}n \tag{28, 29}$$

and e_z denotes the eccentricity in the z-direction of the applied loads measured from the shear center. In what follows this last one will be called load height parameter.

7. Beam forces

In the above expressions, the following 1-D beam forces, in terms of the shell forces, have been defined

$$\begin{aligned}
N &= \int N_{xx} \mathrm{d}s; \qquad M_Y = \int \left(N_{xx}\overline{Z} + M_{xx}\frac{\mathrm{d}Y}{\mathrm{d}s} \right) \mathrm{d}s; \\
M_Z &= \int \left(N_{xx}\overline{Y} - M_{xx}\frac{\mathrm{d}Z}{\mathrm{d}s} \right) \mathrm{d}s; \\
Q_Z &= \int \left(N_{xs}\frac{\mathrm{d}Z}{\mathrm{d}s} + N_{xn}\frac{\mathrm{d}Y}{\mathrm{d}s} \right) \mathrm{d}s; \\
Q_Y &= \int \left(N_{xs}\frac{\mathrm{d}Y}{\mathrm{d}s} - N_{xn}\frac{\mathrm{d}Z}{\mathrm{d}s} \right) \mathrm{d}s; \\
T_w &= \int (N_{xs}(r-\psi) + N_{xn} l)\, \mathrm{d}s; \\
B &= \int (N_{xx}\omega_p - M_{xx} l)\, \mathrm{d}s; \\
T_{sv} &= \int (N_{xs}\psi - 2M_{xs})\, \mathrm{d}s; \\
B_1 &= \int [N_{xx}(Y^2+Z^2) - 2M_{xx} r]\, \mathrm{d}s
\end{aligned} \tag{30}$$

where the integration is carried out over the entire length of the mid-line contour. N corresponds to the axial force, Q_y and Q_z to shear forces, M_y and M_z to bending moments about the y- and z-axis, respectively, B to the bimoment, T_w to the flexural–torsional moment, T_{sv} to the Saint-Venant torsional moment and B_1 to a high-order stress resultant which contributes to the torque.

The relations among the generalized beam forces and the generalized strains characterizing the behavior of the beam are obtained by substituting the expressions (16)–(20) into (23), and the results into (30). This constitutive law can be expressed in terms of a beam stiffness matrix $[K]$ as defined in Appendix B.

8. Lateral buckling considering prebuckling deformation

The stability analysis of bisymmetric thin-walled composite beams is analyzed by taking into account the initial deflection in the prebuckling state (fundamental state). The displacement components in the fundamental state are in the form $\{u, v, \theta_z, w, \theta_y, \phi, \theta\}^t = \{0, 0, 0, w, \theta_y, 0, 0\}^t$, that is to say, the beam deforms in the loading plane. It is reasonable to assume that the fundamental state may be given with sufficient approximation by means of the linearized theory [14].

Ritz's method is used to discretize the variational Eq. (25), and then the buckling loads are obtained by requiring the singularity of the tangent stiffness matrix evaluated at the fundamental state. This procedure leads to a non-linear algebraic problem for the critical loads.

8.1. Simply supported beams

The prebuckling displacements are obtained from the linearized version of Eq. (25). In fact, by neglecting all the non-linear terms in (25), and applying the variational calculus, the differential equations of equilibrium are obtained which are easily solved in a closed form in order to determine the displacements in the loading plane.

For the case of simply supported beams subjected to uniform bending, the prebuckling displacements are given by the following expressions

$$w = \frac{Mo}{2\widehat{EI}_y}(Lx - x^2); \qquad \theta_y = \frac{Mo}{2\widehat{EI}_y}(L - 2x). \tag{31}$$

The variational Eq. (25) is discretized by means of the following functions:

$$\begin{aligned}
v &= v_0 \sin\left(\frac{\pi}{L}x\right); \qquad \theta_z = \theta_{z_0}\cos\left(\frac{\pi}{L}x\right); \\
\phi &= \phi_0 \sin\left(\frac{\pi}{L}x\right); \qquad \theta = \theta_0 \cos\left(\frac{\pi}{L}x\right);
\end{aligned} \tag{32}$$

where $v_0, \theta_{z_0}, \phi_0$ and θ_0 are the associated displacement amplitudes. These approximated displacements correspond to the exact solution of the linearized flexural–torsional buckling problem [14].

To determine the lateral buckling considering prebuckling deformation, expressions (31) and (32) are substituted into (25) and then the tangential stiffness matrix is obtained [22]. This procedure leads to the following expression for the tangential matrix evaluated in the fundamental state.

$$\mathbf{Kt} = \begin{bmatrix}
\frac{\widehat{GS}_y\pi^2}{L^2} & -\frac{\widehat{GS}_y\pi}{L} & 0 & 0 \\
-\frac{\widehat{GS}_y\pi}{L} & \widehat{GS}_y + \widehat{EI}_z\frac{\pi^2}{L^2} & -Mo\left(1 - \frac{\widehat{EI}_z}{\widehat{EI}_y} - \frac{\widehat{GJ}}{4\widehat{EI}_y}\right)\frac{\pi}{L} & \frac{\widehat{EC}_w\pi^2 Mo}{4\widehat{EI}_y L^2} \\
0 & -Mo\left(1 - \frac{\widehat{EI}_z}{\widehat{EI}_y} - \frac{\widehat{GJ}}{4\widehat{EI}_y}\right)\frac{\pi}{L} & -\frac{Mo^2}{\widehat{EI}_y}\left(1 - \frac{\widehat{EI}_z}{\widehat{EI}_y}\right) + (\widehat{GJ} + \widehat{GS}_w)\frac{\pi^2}{L^2} & -\frac{\widehat{GS}_w\pi}{L} \\
0 & \frac{\widehat{EC}_w\pi^2 Mo}{4\widehat{EI}_y L^2} & -\frac{\widehat{GS}_w\pi}{L} & \widehat{GS}_w + \widehat{EC}_w\frac{\pi^2}{L^2}
\end{bmatrix} \tag{33}$$

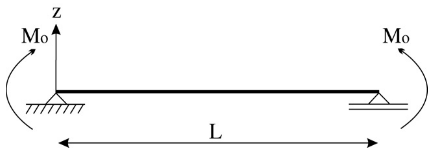

Fig. 2. Simply supported beam subjected to uniform moment.

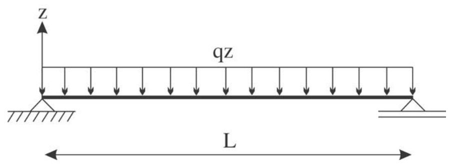

Fig. 3. Simply supported beam subjected to distributed load.

where $\widehat{EI}_y$ is the flexural stiffness, $\widehat{GS}_z$ and $\widehat{GS}_y$ are shear stiffnesses of a composite beam. The definitions of these stiffnesses are given in the Appendix B.

The buckling state is given by the condition of singularity of this matrix [22]:

$$\det(\mathbf{Kt}) = 0. \tag{34}$$

Hence, one obtains a quadratic equation for the external load for the uniform bending case (Fig. 2), the solution of which allows to obtain the critical values.

Following the same procedure and only changing the expression (31) for different loads conditions (distributed load and concentrated load, see Figs. 3 and 4), it is possible to obtain a unified simple formula for the equivalent moment defined as:

$$M_{cr} = \begin{cases} M_{y0} & \text{for uniform bending} \\ q_z L^2/8 & \text{for a uniformly distributed load} \\ & \quad \text{per unit length } q_z \\ PL/4 & \text{for a concentrated force } P \text{ at the} \\ & \quad \text{middle of the span.} \end{cases} \tag{35}$$

The explained technique leads to the following unified expression of the critical moment for the three loading cases analyzed:

$$M_{cr} = C_1 \alpha \widehat{EI}_z \frac{\pi^2}{L^2}\left[-C_2 e_z \alpha + \sqrt{\frac{\widehat{GS}_w \widehat{GJ} + \widehat{EC}_w(\widehat{GS}_w + \widehat{GJ})\frac{\pi^2}{L^2}}{\widehat{EI}_z \frac{\pi^2}{L^2}\left(\widehat{GS}_w + \widehat{EC}_w \frac{\pi^2}{L^2}\right)} + (C_2 e_z \alpha)^2}\,\right] \tag{36}$$

$$\alpha = \left\{\left(1 - \frac{\widehat{EI}_z}{\widehat{EI}_y}\right)\left(1 - \beta\frac{\widehat{GJ}}{\widehat{EI}_y} - \beta\frac{\widehat{EC}_w \widehat{GS}_w \pi^2}{\widehat{EI}_y(\widehat{GS}_w L^2 + \widehat{EC}_w \pi^2)}\right) - \delta\frac{\widehat{EI}_z}{\widehat{GS}_y}\frac{\pi^2}{L^2}\left[1 - \frac{\widehat{GS}_y}{\widehat{GS}_z}\left(0.71 - \frac{\widehat{GS}_y}{\widehat{GS}_z}0.29\right)\right]\right\}^{-\frac{1}{2}} \tag{37}$$

where C_1, C_2, β and δ are approximate constants presented in Table 1.

Expression (36) also gives the corresponding equivalent moments according to the linearized theory (see Appendix C), which does not account for the prebuckling deflection, if one takes $\alpha = 1$ and C_1 and C_2 as indicated in Table 2. These constants are exact from the point of view of the linear theory, for uniform bending and approximate for the other loading cases.

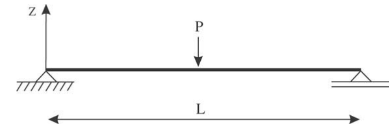

Fig. 4. Simply supported beam subjected to a concentrated load.

Table 1
Parameters in Eqs. (36) and (37)

Simply supported beam	C_1	C_2	β	δ
(a) End moments	1	0	0.5	0
(b) Uniformly distributed load ($M_{cr} = q_z L^2/8$)	1.141	0.459	0.033	0.214
(c) Concentrated force ($M_{cr} = PL/4$)	1.423	0.554	0.076	0.083

Table 2
Parameters in Eq. (36) according to the linearized theory

Simply supported beam	C_1	C_2	α
(a) End moments	1	0	1
(b) Uniformly distributed load ($M_{cr} = q_z L^2/8$)	1.132	0.459	1
(c) Concentrated force ($M_{cr} = PL/4$)	1.366	0.554	1

Therefore, the presence of the α coefficient reveals the dependence of the prebuckling effect with respect to the relation between the bending stiffnesses $\widehat{EI}_z$ and $\widehat{EI}_y$ in the case of uniform bending. For the other two load conditions, α also depends on the bending and shear stiffnesses ($\delta \neq 0$).

As a particular case, neglecting shear deformation, the expression (36) takes the following form for uniform bending:

$$M_{cr} = \frac{\frac{\pi}{L}\sqrt{\widehat{EI}_z\left(\widehat{GJ} + \widehat{EC}_w\frac{\pi^2}{L^2}\right)}}{\sqrt{\left(1 - \frac{\widehat{EI}_z}{\widehat{EI}_y}\right)\left(1 - \frac{\widehat{GJ}}{2\widehat{EI}_y} - \frac{\widehat{EC}_w}{2\widehat{EI}_y}\frac{\pi^2}{L^2}\right)}}. \tag{38}$$

This last expression coincides with the closed-form solution obtained by Pi and Trahair [11] for elastic lateral buckling, of beams made with isotropic materials, considering prebuckling deflections.

8.2. Cantilever beams

In this case, the variational Eq. (25) is discretized by using beam characteristic orthogonal polynomials for the displacements v, θ_z, ϕ and θ, while the displacements w and θ_y (load plane) are adopted as the exact solution of the linearized problem. For this case, the only type of loading considered is a concentrated force applied at the free end of the beam. The corresponding expressions for the prebuckling displacements are given by

$$w = -\frac{P}{\widehat{GS}_z}x + \frac{P}{\widehat{EI}_y}\left(\frac{x^3}{6} - L\frac{x^2}{2}\right);$$

$$\theta_y = \frac{P}{\widehat{EI}_y}\left(\frac{x^2}{2} - Lx\right). \tag{39}$$

The set of orthogonal polynomials which satisfy the geometrical boundary conditions are generated by using the Gram–Schmidt process.

$$U = \sum_{i=1}^{n} c_i \xi_i(x) \tag{40}$$

where U represent each of the displacements v, θ_z, ϕ and θ, and c_i are arbitrary coefficients which are to be determined. The polynomials $\xi_i(x)$ are generated as follows [24]:

$$\xi_2(x) = (x - B_2)\xi_1(x), \ldots, \xi_k(x) = (x - B_k)\xi_{k-1}(x) - C_k\xi_{k-2}(x),$$

$$\text{where } B_k = \frac{\int_0^L x\xi_{k-1}^2(x)\mathrm{d}x}{\int_0^L \xi_{k-1}^2(x)\mathrm{d}x},$$

$$C_k = \frac{\int_0^L x\xi_{k-1}(x)\xi_{k-2}(x)\mathrm{d}x}{\int_0^L \xi_{k-2}^2\mathrm{d}x}. \tag{41}$$

The first member of the orthogonal polynomial $\xi_1(x)$ is chosen as the simplest polynomial (of the least order) that satisfies the boundary conditions.

In order to obtain sufficient accurate results, four terms ($n = 4$) are taken for each one of the flexural–torsional displacements.

Due to the size of the resulting tangential matrix, it is difficult to obtain a simple analytical formula for the critical loads. Therefore these are evaluated numerically from the tangential matrix.

9. Applications and numerical results

The purpose of this section is to apply the present theoretical model in order to study the lateral buckling behavior of thin-walled composite beams. The buckling loads obtained with and without prebuckling deformation are compared, for different load conditions.

In the tables and figures, (LB) denotes values determined by the linear theory (without considering prebuckling deformations) and (NLB) denotes values obtained by means of the present model (accounting for prebuckling deflections).

On the other hand, the influence of shear deformation is analyzed for different laminate stacking sequence. In the following numerical results the shear effect on the thickness $\gamma_{xn}^{(0)}$ has been neglected because its consideration conduces to inaccurate results for thin-walled sections, as explained by Piovan and Cortínez [23]. They showed that the inclusion of the in-thickness shear deformation effect increases erroneously the rigidity instead of flexibilizing the beam behavior.

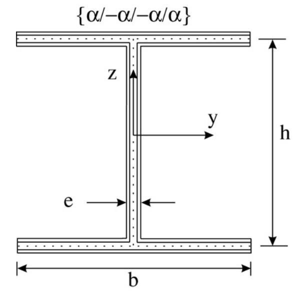

Fig. 5. Analyzed cross-section shape.

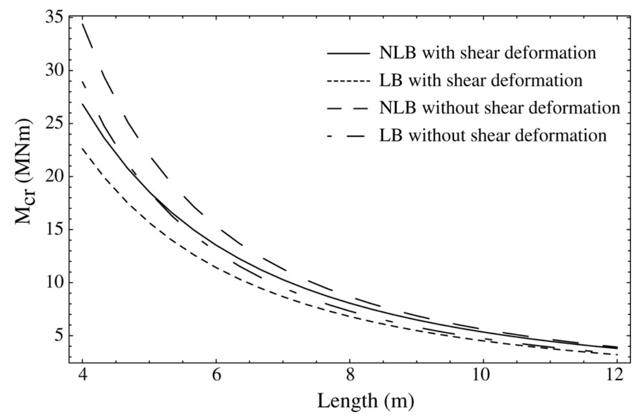

Fig. 6. Buckling loads versus length, lamination {*0/0/0/0*}.

9.1. Simply supported I-beam subjected to uniform moments

The example considered is a simply supported I-beam subjected to uniform bending moment *Mo* applied about its major axis as shown in Fig. 2. The geometrical properties are $h = 0.6$ m, $b = 0.6$ m, $e = 0.03$ m (Fig. 5). The analyzed material is graphite-epoxy (AS4/3501) whose properties are $E_1 = 144$ GPa, $E_2 = 9.65$ GPa, $G_{12} = 4.14$ GPa, $G_{13} = 4.14$ GPa, $G_{23} = 3.45$ GPa, $\nu_{12} = 0.3$, $\nu_{13} = 0.3$, $\nu_{23} = 0.5$.

The buckling loads versus beam lengths are shown in Figs. 6–8, for a sequence of lamination {*0/0/0/0*}, {*0/90/90/0*} and {*45/-45/-45/45*}, respectively. The analytical buckling moments considering and neglecting the prebuckling deflections were calculated by means of expressions (36) and (37) along with Table 1, and by means of expression (36) along with Table 2, respectively.

The buckling moments computed from the linear stability (LB) analysis show a very conservative behavior compared with those computed from the non-linear stability (NLB) model, in fact, considering prebuckling deflections. For example, for a beam length $L = 6$ m and lamination {*0/0/0/0*}, the buckling moments are:

- $M_{cr} = 13.53$ MN m, according to the *Non-Linear Buckling (NLB)* analysis.

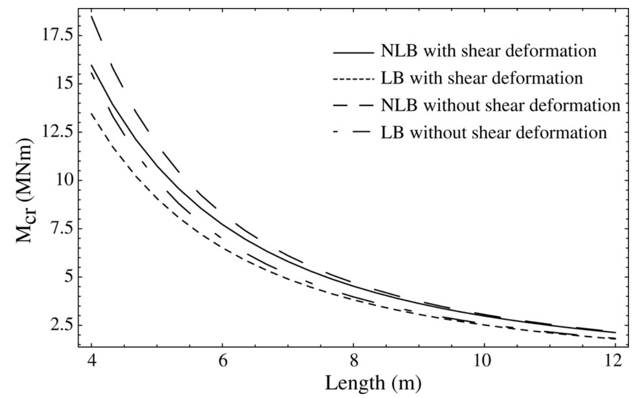

Fig. 7. Buckling loads versus length, lamination {*0/90/90/0*}.

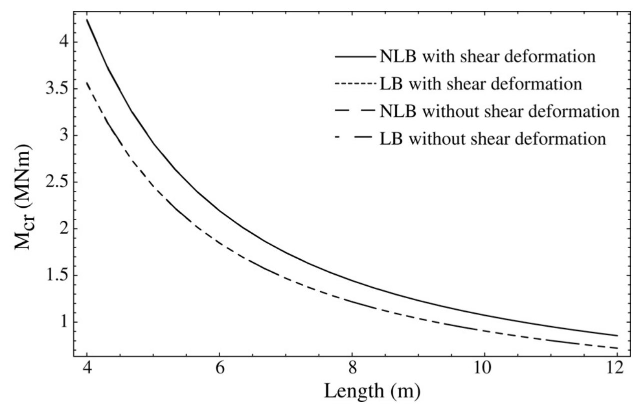

Fig. 8. Buckling loads versus length, lamination {*45/-45/-45/45*}.

- $M_{cr} = 11.42$ MN m, according to the *Linear Buckling (LB)* analysis.

We observe that the effect of the prebuckling deflections is important for all the sequences of lamination and beam lengths. On the other hand, the shear deformation effect is significant for beams with unidirectional fibers and insignificant for the sequence of lamination {*45/-45/-45/45*}. For this last lamination the curves with and without shear deformation coincide for both NLB and LB analysis. Besides, Figs. 6 and 7 show that the buckling moments with and without shear deformation converge as the beam length increases. The shear deformation may significantly reduce the buckling load of short beams. For example, the buckling moments, for a beam length $L = 6$ m and lamination {*0/0/0/0*}, are:

- $M_{cr} = 13.53$ MN m, according to *NLB with shear deformation*.
- $M_{cr} = 15.31$ MN m, according to *NLB without shear deformation*.

9.2. *Simply supported I-beam subjected to distributed load*

In this example a simply supported I-beam under distributed load is considered for three load positions, as shown in Fig. 9. The load can be applied to the top flange (case a), at the shear center (case b), and to the bottom flange (case c). Attention is focused on the importance of the load height parameter effect on the buckling behavior. The geometrical properties and the analyzed material are the same as the previous example.

Figs. 10–12 show comparative results between the non-linear (NLB) and linear (LB) buckling analysis (considering shear effect) in terms of the critical loads, for a sequence of lamination {*0/0/0/0*}, {*0/90/90/0*} and {*45/-45/-45/45*}, respectively. The equivalent buckling moments versus beam lengths are shown for different positions of the applied load over the middle section.

We observe that the lateral buckling strength depends on the load height parameter, and it is higher when the loads are on the bottom flange (case c). The load height parameter effect on the buckling behavior is similar for the different sequences of lamination and beam lengths. As an example, the equivalent buckling moments for a beam length $L = 6$ m are shown in Table 3.

Table 3
Equivalent buckling moment, $L = 6$ m ($M_{cr} \times 10^6$ N m)

Load height	Buckling analysis	{*0/0/0/0*}	{*0/90/90/0*}	{*45/-45/-45/45*}
Top	NLB	8.96	5.19	1.70
	LB	7.89	4.62	1.51
Shear center	NLB	16.59	9.13	2.49
	LB	12.93	7.37	2.09
Bottom	NLB	30.71	16.06	3.66
	LB	21.2	11.76	2.90

One can observe from this table, a noticeable difference between the linear and non-linear buckling model when the load is applied on the bottom flange of the I-beam. This discrepancy can reach a percentage of about 30%. Therefore, the lateral buckling resistance is a function of the initial deflection in the prebuckling state. On other hand, the lamination {*0/0/0/0*} has the higher critical load for the three load positions. For this I-beam the shear deformation effect continues being important and has a similar behavior as in the previous example. For this reason, this effect is not discussed for this load condition.

9.3. *Cantilever beam subjected to end force*

The example considered is a cantilever I-beam subjected to end force for three load positions. The geometrical properties and the analyzed material are the same as the previous example. As an example, the buckling load for a lamination {*0/0/0/0*} and three lengths of beam are shown in Table 4.

One can observe from Table 4, the difference between linear and non-linear buckling analysis is more noticeable for a length of $L = 4$ m and when the load is applied at the shear center of the beam. This discrepancy can reach a percentage of about 36%.

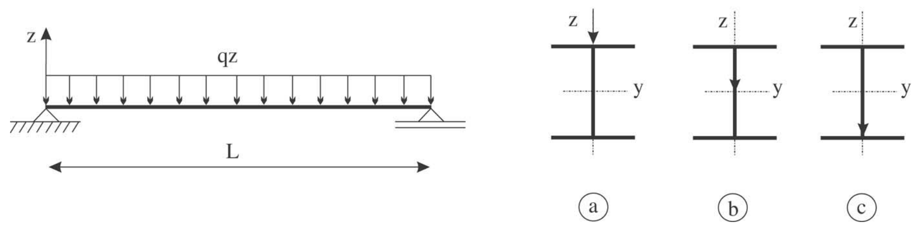

Fig. 9. Different load heights.

Table 4
Buckling load for cantilever beams, {*0/0/0/0*}, $L = 6$ m ($P_{cr} \times 10^6$ N)

Load height	Buckling analysis	$L = 4$ m	$L = 6$ m	$L = 12$ m
Top	NLB	1.87	0.62	0.10
	LB	1.75	0.60	0.10
Shear center	NLB	9.38	2.75	0.39
	LB	5.97	2.30	0.36
Bottom	NLB	11.68	4.11	0.67
	LB	10.09	4.06	0.65

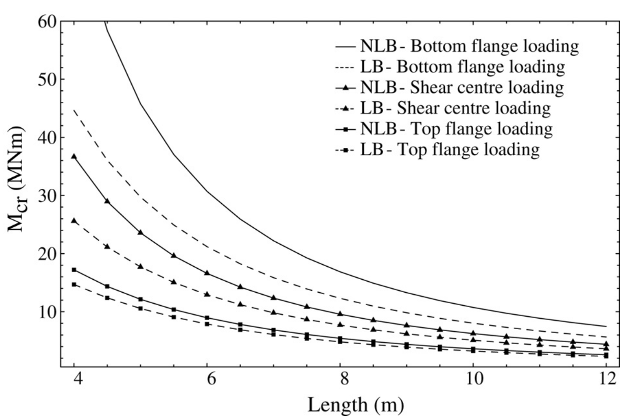

Fig. 10. Buckling loads versus length, lamination {*0/0/0/0*}.

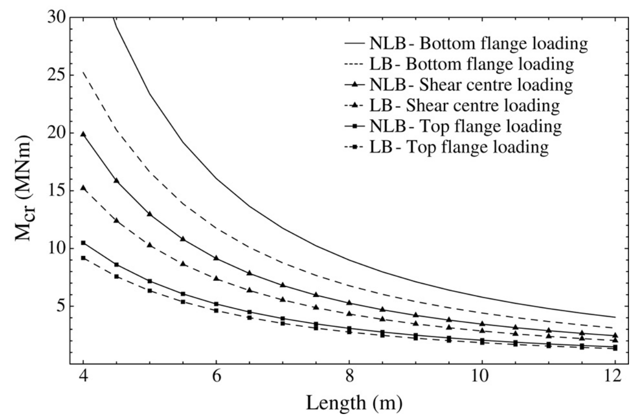

Fig. 11. Buckling loads versus length, lamination {*0/90/90/0*}.

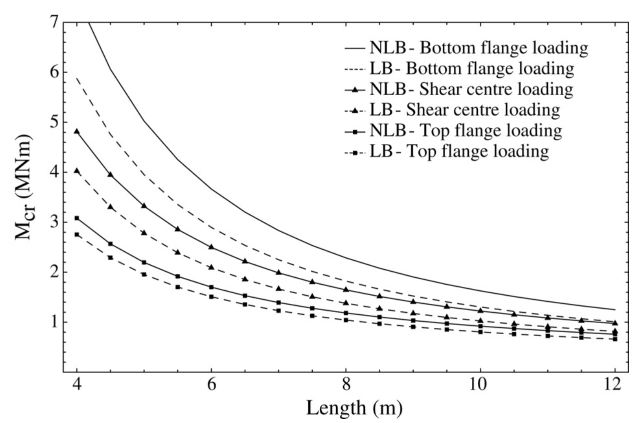

Fig. 12. Buckling loads versus length, lamination {*45/-45/-45/45*}.

For verification purpose, an isotropic cantilever I-beam subjected to a vertical end force P is considered. Two different positions of the applied load are examined: load at the top flange and load at the shear center. The geometrical properties are $h = 0.0724$ m, $b = 0.0315$ m, $t_f = 0.0031$ m, $t_w = 0.0022$ m (Fig. 13). The material properties are assumed to be: $E = 65{,}120$ MPa, $G = 25{,}965$ MPa. This example was investigated experimentally and theoretically by Anderson and Trahair [12] and also studied by Pi and Trahair [11] and Lin and Hsiao [25] using the finite element method. The present buckling loads, obtained by using $n = 4$ in expression (40), are shown in Table 5 together with those given in [11,12,25]. It is seen that the present solutions are in good agreement with those obtained by the experimental results.

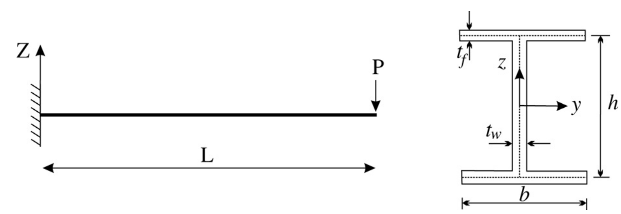

Fig. 13. Cantilever beam subjected to end force.

Table 5
Comparison of buckling load for a cantilever I-beam, P_{cr} (N)

L (m)	Load height	Exp. [12]	Theory [12]	FEM [11]	FEM [25]	Present
1.65	Top	256.7	252.8	251.4	250.0	**248.0**
	Shear center	323.5	330.2	338.5	331.4	**323.4**
1.27	Top	405.8	421.0	409.6	408.3	**405.5**
	Shear center	597.2	619.4	630.9	614.3	**591.8**

9.4. Comparison of the present model against a moderate rotation theory

The purpose of this example is to show the effect of the degree of non-linearity adopted in the displacement field (4) on the lateral buckling loads. A simply supported I-beam subjected to a transverse force P at the middle of the span is considered, as shown in Fig. 4. Three different positions of the applied load are examined: load at the top flange, load at the shear center and load at the bottom flange. The geometrical properties are $h = 0.05$ m, $b = 0.05$ m, $e = 0.003$ m. The analyzed material is glass-epoxy (S2) whose properties are $E_1 = 48.3$ GPa, $E_2 = 19.8$ GPa, $G_{12} = 8.96$ GPa, $G_{13} = 8.96$ GPa, $G_{23} = 6.19$ GPa, $\nu_{12} = 0.27$, $\nu_{13} = 0.27$, $\nu_{23} = 0.6$.

In Table 6, the results by the present closed-form solution (36) and (37) are compared with those obtained by using a second-order displacement field by Fraternali and Feo [18].

Table 6
Critical values of the load multiplier (λ) for simply supported beams

Load height	Buckling analysis	Present model	Fraternali and Feo [18]
Top	LB	17.12	16.61
	NLB	20.05	21.75
Shear center	LB	25.58	25.59
	NLB	32.48	44.34
Bottom	LB	38.22	39.17
	NLB	52.63	88.6

Fraternali et al. investigated the post-buckling behavior of thin-walled composite beams by using a second-order displacement field (see Appendix A) obtained through a second-order rotation matrix. The use of the second-order rotation matrix in these studies may lead to the loss of some significant terms in the non-linear strains and in the tangential matrix, thus some inaccurate approximations in the coupling between displacements, rotations and their derivates [11].

In the Fraternali and Feo [18] example, the results were obtained by employing a mesh of 30 two-node finite elements over the beam length. The following scaling factor of the load Q_z is used:

$$\lambda = \frac{PL^2}{\sqrt{\widehat{EI}_z \widehat{GJ}}}.$$

Quoted results refer to a value of the dimensionless ratio $\alpha = \widehat{GJ}L^2/\widehat{EC}_w = 8$.

It is seen that the results by the second-order approximation overestimates the maximum load-carrying capacity, and this effect is more noticeable when the load is applied on the bottom flange.

10. Conclusions

In this paper a geometrically non-linear theory for thin-walled composite beams is presented. The theory is formulated in the context of large displacements and rotations, through the adoption of a shear deformable displacement field (accounting for bending and warping shear) considering moderate bending rotations and large twist. The theory accounts for bisymmetric cross-sections either open or closed.

The Ritz method was applied in order to obtain an approximate tangential matrix that allows to determine the critical loads considering prebuckling deflections.

From some numerical examples studied, it is found that the agreement between the buckling loads of the present study (considering prebuckling effect) and those from experimental studies given in the literature is very good. In the case of simply supported ends a practical general formula was obtained for determining the critical loads of lateral buckling for bisymmetrical thin-walled beams. This formula takes into account the effects of prebuckling and shear deformation for beams subjected to concentrated end moments, concentrated forces, or uniformly distributed loads.

From the numerical studies, it has been established that the buckling loads obtained from the linear theory are very conservative in some cases.

On the other hand, the shear deformation effect has been investigated. For the analyzed cases, this effect may be significant for short beams, in particular when one of the material axes coincides with the beam axis. In the case of lateral loads, the prebuckling influence is highly dependent on the load height parameter. Moreover, shear effect may be higher for other boundary conditions such as clamped–clamped conditions [14,19]. These cases are to be investigated in a future work.

Acknowledgments

The present study was sponsored by Secretaría de Ciencia y Tecnología, Universidad Tecnológica Nacional, and by CONICET.

Appendix A

The following displacement field corresponding to the one developed by Fraternali and Feo [18] but referred to our

Cartesian co-ordinate system is given by (see Fig. 1):

$$\begin{aligned} u_x &= u_o - v'\bar{y} - w'\bar{z} + \phi v' z - \phi w' y \\ &\quad + \omega\left[\phi' - \frac{1}{2}\left(w''v' - w'v''\right)\right] \\ u_y &= v - \phi z + \frac{1}{2}(-\phi^2 y - v'^2\bar{y} - v'w'\bar{z}) \\ u_z &= w + \phi y + \frac{1}{2}(-\phi^2 z - w'^2\bar{z} - v'w'\bar{y}). \end{aligned} \tag{A.1}$$

This last is based on the principle of semitangential rotation defined by Argyris [26] to avoid the difficulty due to the noncommutative nature of rotations. A remarkable characteristic of this displacement field is the calculation of the warping function carried out on the basis of two assumptions:

$$\varepsilon_{xn} = 0; \qquad \varepsilon_{xs}|_{n=0} = 0. \tag{A.2}$$

Finally, these last assumptions are not taken into account in the expression (4).

Appendix B

The constitutive law for a bisymmetric beam is defined in the following form:

$$\{f_g\} = [K]\{\Delta\} \tag{B.1}$$

$$\{f_g\} = [N\ M_y\ M_z\ B\ Q_y\ Q_z\ T_w\ T_{sv}\ B_1]^{\mathrm{T}} \tag{B.2}$$

$$\{\Delta\} = [\varepsilon_{D1}\ \varepsilon_{D2}\ \varepsilon_{D3}\ \varepsilon_{D4}\ \varepsilon_{D5}\ \varepsilon_{D6}\ \varepsilon_{D7}\ \varepsilon_{D8}\ \varepsilon_{D9}]^{\mathrm{T}} \tag{B.3}$$

where $\{f_g\}$ is the vector of generalized forces, $\{\Delta\}$ is the vector of the generalized strains and $[K]$ is a symmetric matrix (9×9).

$$\begin{aligned} \varepsilon_{D1} &= u_o' + \frac{1}{2}(v'^2 + w'^2); \\ \varepsilon_{D2} &= -\theta_y' \cos\phi + \theta_z' \sin\phi; \\ \varepsilon_{D3} &= -\theta_z' \cos\phi - \theta_y' \sin\phi; \\ \varepsilon_{D4} &= \theta' - \frac{1}{2}(\theta_z\theta_y'' - \theta_y\theta_z''); \\ \varepsilon_{D5} &= (v' - \theta_z)\cos\phi + (w' - \theta_y)\sin\phi; \\ \varepsilon_{D6} &= (w' - \theta_y)\cos\phi - (v' - \theta_z)\sin\phi; \\ \varepsilon_{D7} &= \phi' - \theta; \\ \varepsilon_{D8} &= \phi' - \frac{1}{2}(\theta_z\theta_y' - \theta_y\theta_z'); \\ \varepsilon_{D9} &= \frac{1}{2}\phi'^2; \end{aligned} \tag{B.4}$$

$$K = \begin{bmatrix} \widehat{EA} & 0 & 0 & 0 & 0 & 0 & 0 & 0 & \widehat{EI}_0 \\ 0 & \widehat{EI}_y & 0 & 0 & 0 & 0 & 0 & 0 & 0 \\ 0 & 0 & \widehat{EI}_z & 0 & 0 & 0 & 0 & 0 & 0 \\ 0 & 0 & 0 & \widehat{EC}_w & 0 & 0 & 0 & 0 & 0 \\ 0 & 0 & 0 & 0 & \widehat{GS}_y & 0 & 0 & 0 & 0 \\ 0 & 0 & 0 & 0 & 0 & \widehat{GS}_z & 0 & 0 & 0 \\ 0 & 0 & 0 & 0 & 0 & 0 & \widehat{GS}_w & 0 & 0 \\ 0 & 0 & 0 & 0 & 0 & 0 & 0 & \widehat{GJ} & 0 \\ \widehat{EI}_0 & 0 & 0 & 0 & 0 & 0 & 0 & 0 & \widehat{EI}_R \end{bmatrix} \tag{B.5}$$

The elements of the symmetric matrix $[K]$ are given by the following contour integrals:

$$\begin{aligned} \widehat{EA} &= \int \overline{A}_{11}\mathrm{d}s; \\ \widehat{EI}_y &= \int (\overline{A}_{11}Z^2 + \overline{D}_{11}Y'^2)\mathrm{d}s; \\ \widehat{EI}_z &= \int (\overline{A}_{11}Y^2 + \overline{D}_{11}Z'^2)\mathrm{d}s; \\ \widehat{EI}_w &= \int (\overline{A}_{11}\omega_p^2 + \overline{D}_{11}l^2)\mathrm{d}s; \\ \widehat{GS}_y &= \int (\overline{A}_{55}Z'^2 + \overline{A}_{66}Y'^2)\mathrm{d}s; \\ \widehat{GS}_z &= \int (\overline{A}_{55}Y'^2 + \overline{A}_{66}Z'^2)\mathrm{d}s; \\ \widehat{GJ} &= \int (\overline{A}_{66}\psi^2 + 4\overline{D}_{66})\mathrm{d}s; \\ \widehat{EI}_R &= \int [\overline{A}_{11}(Y^2 + Z^2)^2 + 4\overline{D}_{11}r^2]\mathrm{d}s; \\ \widehat{EI}_0 &= \int \overline{A}_{11}(Y^2 + Z^2)\mathrm{d}s. \end{aligned} \tag{B.6}$$

where $Y' = \frac{\mathrm{d}Y}{\mathrm{d}s}$; $Z' = \frac{\mathrm{d}Z}{\mathrm{d}s}$.

Appendix C. Linearized lateral buckling of simply supported I-beams

The stability analysis of simply supported doubly symmetric thin-walled composite beams subjected to concentrated end moments, concentrated forces, or uniformly distributed load, is analyzed. The linearized governing equations may be obtained from Eq. (25) applying the usual concepts of variational calculus and linearizing the resultant expressions. This procedure leads to the following equations [14]:

$$N' = 0 \tag{C.1}$$

$$M_y' - Q_z = 0 \tag{C.2}$$

$$-Q_z' = q_z \tag{C.3}$$

$$M_z' - Q_y - [M_y\phi]' = 0 \tag{C.4}$$

$$-Q_y' = 0 \tag{C.5}$$

$$-B' - T_w = 0 \tag{C.6}$$

$$-T_w' - T_{sv}' + M_y\theta_z' = -q_z z_0\phi. \tag{C.7}$$

Eq. (C.1) corresponding to the equilibrium in the axial direction is uncoupled from the rest and it is not of interest here. Eqs. (C.2) and (C.3) correspond to the classical bending of the beam before buckling. The lateral buckling is governed by Eqs. (C.4)–(C.7). In this case, buckling is assumed to be independent of the prebuckling deflections (classical analysis).

Eqs. (C.4)–(C.7) are coupled. However, in the case of a simply supported beam, Eq. (C.4) can be derivated once to obtain the following expression:

$$M_z'' - Q_y' - [M_y \phi]'' = 0. \tag{C.8}$$

With the consideration of (C.5), the last one may be written as

$$[M_z - M_y \phi]'' = 0. \tag{C.9}$$

Integrating twice and taking into account the linearized constitutive equation for the bending moment M_z (see Appendix B) and the boundary conditions, one arrives to:

$$-\widehat{EI}_z \theta_z' - \phi M_y = 0. \tag{C.10}$$

Substituting this last expression along with the linearized constitutive equations for T_w, T_{sv} and B (see Appendix B) into (C.6) and (C.7), one arrives to:

$$-\widehat{EC}_w \theta'' - \widehat{GS}_w (\phi' - \theta) = 0 \tag{C.11}$$

$$-\widehat{GS}_w (\phi'' - \theta') - \widehat{GJ} \phi'' - \frac{M_y^2}{\widehat{EI}_z} \phi = -q_z e_z \phi. \tag{C.12}$$

Ritz's method is used for computing analytical solutions of these last equations. The twisting and warping displacements are approximated by means of the following functions, which are compatible with the boundary conditions of the beam:

$$\phi = \phi_0 \sin\left(\frac{\pi}{L} x\right); \qquad \theta = \theta_0 \cos\left(\frac{\pi}{L} x\right); \tag{C.13}$$

where ϕ_0 and θ_0 are the associated displacement amplitudes. Using this method and after integration along the beam length according to the adopted functions for the displacements, the buckling loads or equivalent buckling moments are given by obtaining the roots of a quadratic equation.

Using this procedure, it is possible to obtain a unified simple formula for the equivalent moment for different loads. This formula may be expressed as indicated in (36) with the constants defined as in Table 2.

References

[1] Timoshenko SP, Gere JM. Theory of elastic stability. 2nd ed. New York: McGraw-Hill; 1961.

[2] Bleich F. Buckling strength of metal structures. New York: McGraw-Hill; 1952.

[3] Chajes A. Principle of structural stability theory. Englewood Cliffs (NJ): Prentice-Hall; 1952.

[4] Vlasov VZ. Thin walled elastic beams. Jerusalem: Israel Program for Scientific Translation; 1961.

[5] Goodier JN. The buckling of compressed bars by torsion and flexure, Bulletin 27. Cornell University Engineering Experimental Station; 1941.

[6] Wang CM, Wang CY, Reddy JN. Exact solutions for buckling of structural members. Boca Raton (FL): CRC Press; 2004.

[7] Sapkás A, Kollár LP. Lateral–torsional buckling of composite beams. Int J Solids Struct 2002;39:2939–63.

[8] Lee J, Kim SE, Hong K. Lateral buckling of I-section composite beams. Eng Struct 2002;24:955–64.

[9] Trahair NS. Flexural–torsional buckling of structures. Boca Raton (FL): CRC Press; 1993.

[10] Vacharajittiphan P, Woolcock ST, Trahair NS. Effect of in-plane deformation on lateral buckling. J Struct Mech 1974;3(1):29–60.

[11] Pi YL, Trahair NS. Prebuckling deflections and lateral buckling. II: applications. J Struct Engrg ASCE 1992;118(11):2967–85.

[12] Anderson JM, Trahair NS. Stability of monosymmetric beams and cantilevers. J Struct Div ASCE 1972;98:269–86.

[13] Mohri F, Azrar L, Potier-Ferry M. Lateral post-buckling analysis of thin-walled open sections beams. Thin Walled Struct 2002;40:1013–36.

[14] Cortínez VH, Piovan MT. Vibration and buckling of composite thin-walled beams with shear deformability. J Sound Vibration 2002;258(4):701–23.

[15] Barbero EJ. Introduction to composite material design. Taylor and Francis Inc; 1999.

[16] Reddy JN. Mechanics of laminated composite plates and shells: theory and analysis. 2nd ed. Boca Raton (FL): CRC Press; 2004.

[17] Reddy JN. Energy principles and variational methods in applied mechanics. 2nd ed. NY: John Wiley; 2002.

[18] Fraternali F, Feo L. On a moderate rotation theory of thin-walled composite beams. Composites B 2000;31:141–58.

[19] Cortínez VH, Rossi RE. Dynamics of shear deformable thin-walled open beams subjected to initial stresses. Rev Internac Métod Numér Cálc Diseñ Ingr 1998;14(3):293–316.

[20] Krenk S, Gunneskov O. Statics of thin-walled pre-twisted beams. Int J Numer Methods Eng 1981;17:1407–26.

[21] Washizu K. Variational methods in elasticity and plasticity. Pergamon Press; 1968.

[22] Bazant ZP, Cedolin L. Stability of structures: elastic, inelastic, fracture, and damage theories. Mineola (NY): Dover Publication Inc.; 2003.

[23] Piovan MT, Cortínez VH. Transverse shear deformability in the dynamics of thin-walled composite beams: consistency of different approaches. J Sound Vibration [in press].

[24] Bhat RB. Transverse vibrations of a rotating uniform cantilever beam with tip mass as predicted by using beam characteristic orthogonal polynomials in the Rayleigh–Ritz method. J Sound Vibration 1986;105(2):199–210.

[25] Lin WL, Hsiao KM. Co-rotational formulation for geometric nonlinear analysis of doubly symmetric thin-walled beams. Comput Methods Appl Mech Engrg 2001;190:567–94.

[26] Argyris JH. Comput Methods Appl Mech Engrg 1982;32:85–155.